Magnetospheres of stars (and giant planets)

Interaction of wind and magnetic field

Jiří Krtička

Masaryk University

Introduction

Interaction of wind and magnetic field

Stellar winds of hot star are ionized $\Rightarrow$ wind flows along the magnetic field-lines.

Idealized MHD ($\sigma \to \infty$):

$$\frac{\partial \boldsymbol{B}}{\partial t} = \nabla \times (\boldsymbol{v} \times \boldsymbol{B}) \Rightarrow \nabla \times (\boldsymbol{v} \times \boldsymbol{B}) = 0 \text{ for } \frac{\partial \boldsymbol{B}}{\partial t} = 0.$$

About 10% of OB stars have strong (measurable) magnetic fields with surface strengths of the order of 0.1 – 10 kG (Aurière at al. 2007, Romanyuk 2007): *magnetic O stars* (e.g., θ^1 Ori C, HD 191612, Donati et al. 2002, 2006) and *chemically peculiar stars* (He-rich and He-poor: σ Ori E, CU Vir, Oksala et al. 2015, Kochukhov et al. 2014).

What is the influence of the magnetic field on the outflow?

Wind magnetic confinement parameter η_*

Magnetic confinement parameter η_*

The effect of the the magnetic field is given by the ratio of the magnetic field density and wind kinetic energy density:

$$\eta = \frac{\frac{1}{8\pi} B^2}{\frac{1}{2}\rho v^2}.$$

With wind *mass-loss rate* $\dot{M} = 4\pi r^2 \rho v$ and replacing $B = B_{\mathrm{eq}}$ with equatorial field strength, $r = R_*$ with the stellar radius, and $v = v_\infty$ with the terminal velocity we derive

$$\eta_* = \frac{B_{\mathrm{eq}}^2 R_*^2}{\dot{M} v_\infty},$$

which is wind magnetic confinement parameter (ud-Doula & Owocki 2002).

Weak confinement $\eta_* \lesssim 1$

$\eta_* \lesssim 1$: the wind energy density dominates over the magnetic field energy density. The magnetic fields opens up. The wind flows radially.

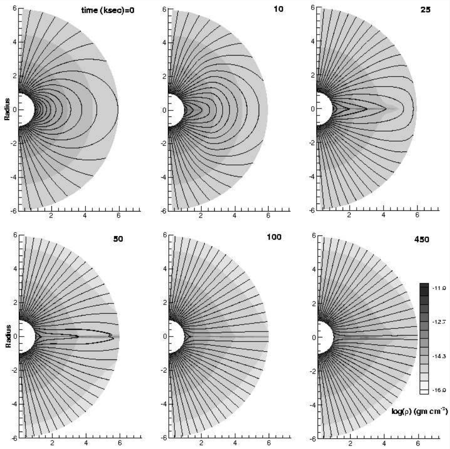

(ud-Doula & Owocki 2002)

Strong confinement $\eta_* \gtrsim 1$

$\eta_* \gtrsim 1$: the magnetic field energy density dominates over the wind energy density. Wind trapped by the magnetic field, collision of wind flow from opposite footpoints of magnetic loops: magnetically confined wind shocks (Babel & Montmerle 1997).

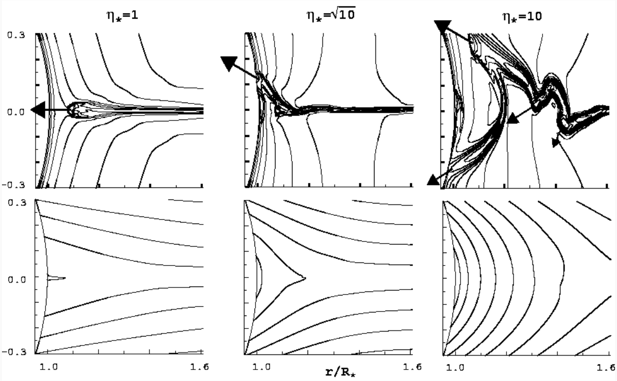

Arrows denote infall (the flow is not stable, ud-Doula & Owocki 2002).

Magnetic confinement parameter η_* in real stars

$$\eta_* = \frac{B_{\mathrm{eq}}^2 R_*^2}{\dot{M} v_\infty}$$

- strong winds in massive stars (e.g., HD 191612): for $\dot{M} \approx 10^{-6}\,\mathrm{M}_\odot\,\mathrm{yr}^{-1}$ the magnetic field of the order of 100 G is needed for strong confinement
- weak winds in cool stars (e.g., Sun): for $\dot{M} \approx 10^{-14}\,\mathrm{M}_\odot\,\mathrm{yr}^{-1}$ the magnetic field of the order of 1 G is enough for strong confinement (e.g., corona)

Alfvén radius

Reshuffling the confinement parameter in terms of Alfvén speed v_A

$$\eta = \frac{\frac{1}{8\pi}B^2}{\frac{1}{2}\rho v^2} = \frac{\frac{B^2}{4\pi\rho}}{v^2} = \frac{v_\mathrm{A}^2}{v^2} = \frac{1}{M_\mathrm{A}^2}$$

$\Rightarrow$ inverse of the confinement parameter represents the square of the Alfvénic Mach number $M_\mathrm{A} = v/v_\mathrm{A}$.

The radial dependence (with dipolar field with $B \sim r^{-3}$ and $v \to v_\infty$)

$$\eta = \frac{\frac{1}{8\pi}B^2}{\frac{1}{2}\rho v^2}\frac{r^2}{r^2} = \frac{B^2 r^2}{\dot{M} v} \sim r^{-4}$$

$\Rightarrow$ the wind speed overcomes the Alfvén speed ($\eta = M_\mathrm{A} = 1$) at Alfvén radius R_A, from fits of numerical simulation (ud-Doula et al. 2008)

$$\frac{R_\mathrm{A}}{R_*} \approx 0.3 + (\eta_* + 0.25)^{1/4}$$

Wind quenching by magnetic confinement

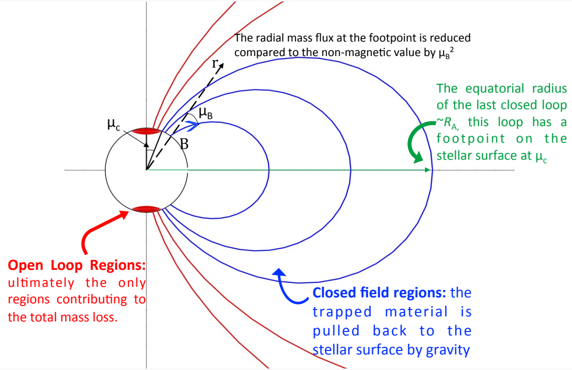

Closed loops: $M_A < 1$ everywhere. The last closed loop: $M_A = 1$ at the loop apex. Wind leaves the star on open loops that have $M_A > 1$ at the loop apex $\Rightarrow$ significant reduction of the net mass-loss rate: *wind quenching*.

(Babel & Montmerle 1997, ud-Doula & Owocki 2008, Petit et al. 2017)

Wind quenching by magnetic confinement

From the equation for the dipolar field $r = R_{\rm apex} \sin\theta^2$, where $R_{\rm apex}$ is the apex radius and θ is the colatitude, equating $R_{\rm apex} = R_{\rm A}$ gives that the magnetic field is open for $\theta < \theta_{\rm A}$ given by

$$\theta_{\rm A} = \arcsin\sqrt{\frac{R_*}{R_{\rm A}}}.$$

Numerical simulations (ud-Doula et al. 2008) give slightly lower maximum radius of closed magnetic loop as $R_{\rm c} \approx R_* + 0.7(R_{\rm A} - R_*)$.

The escaping wind fraction

$$f_B = \frac{\dot{M}}{\dot{M}_{B=0}} = \int_0^{\theta_{\rm c}} \sin\theta \,{\rm d}\theta = 1 - \cos\theta_{\rm c} = 1 - \sqrt{1 - \frac{R_*}{R_{\rm c}}}$$

is of the order of $0.01 - 0.1$ for strong fields.

Magnetic hot stars may be progenitors of massive binary black holes (Petit et al. 2017), which were detected as gravitational wave sources (Abbott et al. 2016).

The effect on mass flux

Magnetic field influences also the mass flux from the stellar photosphere. The spherically symmetric stationary equation of motion has the form of

$$(\boldsymbol{v} \cdot \nabla)\boldsymbol{v} = -g_* \hat{\boldsymbol{r}} \; + \; g_{\mathrm{rad}} \hat{\boldsymbol{r}},$$

where we neglected the gas pressure term, $g_* = GM(1-\Gamma)/r^2$, Γ is the Eddington factor, and g_{rad} is the acceleration due to the lines,

$$g_{\mathrm{rad}} = \frac{1}{1-\alpha} \frac{\kappa_{\mathrm{e}} F \bar{Q}}{c} \left(\frac{\mathrm{d}v/\mathrm{d}r}{\rho c \bar{Q} \kappa_{\mathrm{e}}} \right)^{\alpha}.$$

Here α and $\bar{Q}$ are line force parameters (Castor, Abbott, & Klein 1975, Gayley 1995) and F is the total flux at radius r.

The effect on mass flux

In magnetic field the wind flows along the magnetic field along the direction $\hat{\boldsymbol{s}}$ tilted by an angle θ_B with respect to the vertical direction $\hat{\boldsymbol{z}}$. Equation of motion has in the plane parallel case the form of

$$(\boldsymbol{v} \cdot \nabla)(\hat{\boldsymbol{s}} \cdot \boldsymbol{v}) = -g_*(\hat{\boldsymbol{s}} \cdot \hat{\boldsymbol{z}}) \;+\; g_{\mathrm{rad}}(\hat{\boldsymbol{s}} \cdot \hat{\boldsymbol{z}}).$$

With $\boldsymbol{v} = v_s\hat{\boldsymbol{s}}$ we derive $(\boldsymbol{v} \cdot \nabla)(\hat{\boldsymbol{s}} \cdot \boldsymbol{v}) = v_s(\hat{\boldsymbol{s}} \cdot \nabla)(v_s) =$
$= \mu_B v_s \frac{\partial v_s}{\partial z} + \sqrt{1-\mu_B^2}\, v_s \frac{\partial v_s}{\partial x} = \mu_B v_s \frac{\partial v_s}{\partial z}$ without horizontal velocity variations ($\frac{\partial v_s}{\partial x} = 0$). The radiative force is

$$\begin{aligned}
(\hat{\boldsymbol{s}} \cdot \hat{\boldsymbol{z}}) g_{\mathrm{rad}} &= \frac{1}{1-\alpha}(\hat{\boldsymbol{s}} \cdot \hat{\boldsymbol{z}})\frac{\kappa_{\mathrm{e}} F \bar{Q}}{c}\left(\frac{\hat{\boldsymbol{z}} \cdot \nabla(\hat{\boldsymbol{z}} \cdot \boldsymbol{v})}{\rho c \bar{Q} \kappa_{\mathrm{e}}}\right)^{\alpha} \\
&= \frac{\mu_B}{1-\alpha}\frac{\kappa_{\mathrm{e}} F \bar{Q}}{c}\left(\frac{\mu_B \partial v_s/\partial z}{\rho c \bar{Q} \kappa_{\mathrm{e}}}\right)^{\alpha} \\
&= \frac{\mu_B}{1-\alpha}\frac{\kappa_{\mathrm{e}} F \bar{Q}}{c}\left(\frac{\mu_B^2 v_s \partial v_s/\partial z}{\dot{m}_r c \bar{Q} \kappa_{\mathrm{e}}}\right)^{\alpha},
\end{aligned}$$

where the *radial* mass flux is $\dot{m}_r = \mu_B \rho v_s$.

The effect on mass flux

Substituting $w' = (v_s/g_*)\partial v_s/\partial z$ the momentum equation is

$$w' = -1 + C\mu_B^{2\alpha}(w')^{\alpha}$$

with

$$C = \frac{1}{1-\alpha}\left(\frac{F}{\dot{m}_r c^2}\right)^{\alpha}\left(\frac{\bar{Q}\Gamma}{1-\Gamma}\right)^{1-\alpha}.$$

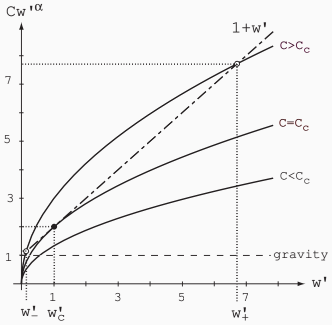

Equation has two, one, or no solution according to the value of C ($\dot{m}_r$).

Maximum mass-loss rate for tanget of the radiative force equal to one: $\alpha C_c \mu_B^{2\alpha} {w'_c}^{\alpha-1} = 1$, from the momentum equation $w'_c = \alpha/(1-\alpha)$ and $C_c = \alpha^{-\alpha}(1-\alpha)^{\alpha-1}\mu_B^{-2\alpha}$ and

$$\dot{m}_r = \mu_B^2 \dot{m}_{\mathrm{CAK}},$$

where m_{CAK} is the mass-flux for $\mu_B = 1$ (Owocki & ud-Doula 2004).

The effect of stellar rotation

Kepler corotation radius

Non-degenerate stars: in the strong confinement limit $\eta_* \gg 1$ the magnetosphere rotates as a rigid body close to the star.

Kepler corrotation radius: the velocity of the corotationg matter equal to the Kepler (orbital) velocity:

$$\sqrt{\frac{GM}{R_\mathsf{K}}} = \Omega R_\mathsf{K} = \frac{V_\mathrm{rot}}{R_*} R_\mathsf{K} \rightarrow R_\mathsf{K} = \left(\frac{GM}{V_\mathrm{rot}^2}\right)^{1/3}.$$

In terms of *orbital rotation fraction* W:

$$W = \frac{V_\mathrm{rot}}{V_\mathrm{orb}} = \frac{V_\mathrm{rot}}{\sqrt{\frac{GM}{R_*}}} \rightarrow R_\mathsf{K} = W^{-2/3} R_*.$$

The material may be centrifugally supported for $r > R_\mathsf{K}$.

Dynamical versus centrifugal magnetospheres

dynamical magnetosphere $R_{\mathsf{A}} < R_{\mathsf{K}}$: material trapped in the magnetosphere falls back to the surface (as in the case without rotation)

centrifugal magnetosphere $R_{\mathsf{A}} > R_{\mathsf{K}}$: material is supported against gravity by the magnetically enforced corotation: material can stay in equilibrium in magnetosphere

Centrifugal magnetospheres

The effective potential in the frame that corotates with the star

$$\Phi_{\text{eff}} = -\frac{GM}{r} - \frac{1}{2}\Omega^2 r^2 \sin^2\theta$$

in dimensionless units $\xi = r/R_{\text{K}}$ is

$$\Psi_{\text{eff}} = \frac{R_{\text{K}}}{GM}\Phi_{\text{eff}} = -\frac{1}{\xi} - \frac{1}{2}\xi^2 \sin^2\theta.$$

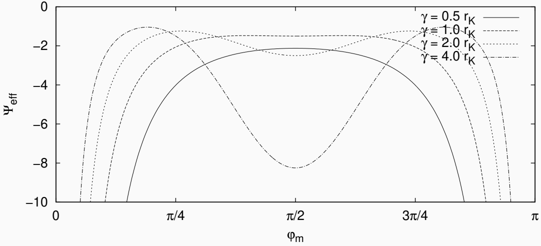

Minima of the potential along the field line ⇒ accumulation of matter (Townsend & Owocki 2005, Prvák 2011).

Centrifugal magnetospheres

The effective potential in the frame that corotates with the star

$$\Phi_{\text{eff}} = -\frac{GM}{r} - \frac{1}{2}\Omega^2 r^2 \sin^2\theta$$

in dimensionless units $\xi = r/R_{\text{K}}$ is

$$\Psi_{\text{eff}} = \frac{R_{\text{K}}}{GM}\Phi_{\text{eff}} = -\frac{1}{\xi} - \frac{1}{2}\xi^2 \sin^2\theta.$$

Minima of the potential along the field line $\Rightarrow$ accumulation of matter (Townsend & Owocki 2005, Prvák 2011).

$\Rightarrow$ hydrostatic hydrostatic equilibrium along the field line

$$\rho = \rho_0 \left(-\mu \frac{\Phi_{\text{eff}} - \Phi_0}{kT}\right)$$

$\Rightarrow$ *rigidly rotating magnetosphere (RMM)* model

Showcase of RMM model: σ Ori E: magnetosphere

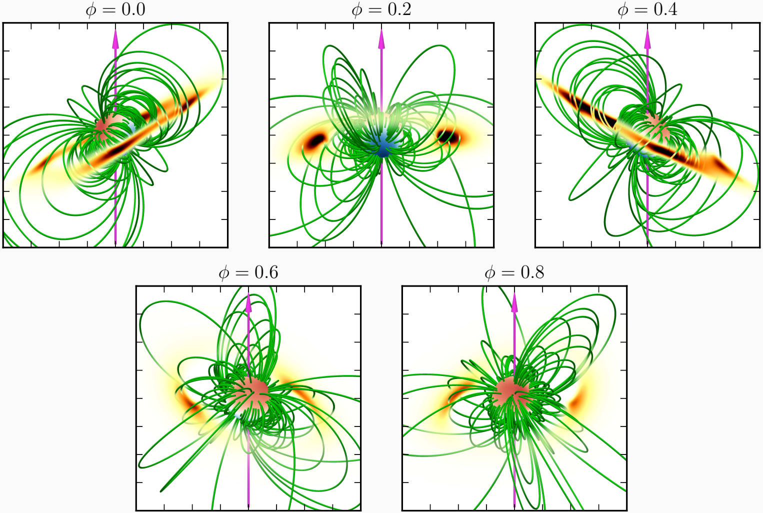

(Oskala et al. 2015)

Showcase of RMM model: σ Ori E: Hα line

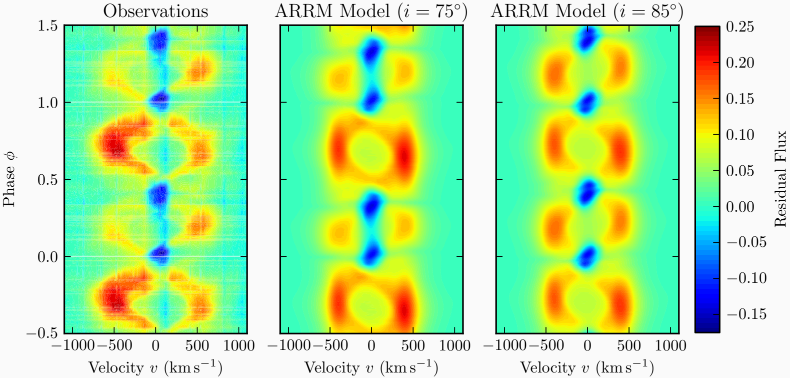

(Oskala et al. 2015)

Showcase of RMM model: σ Ori E: optical variability

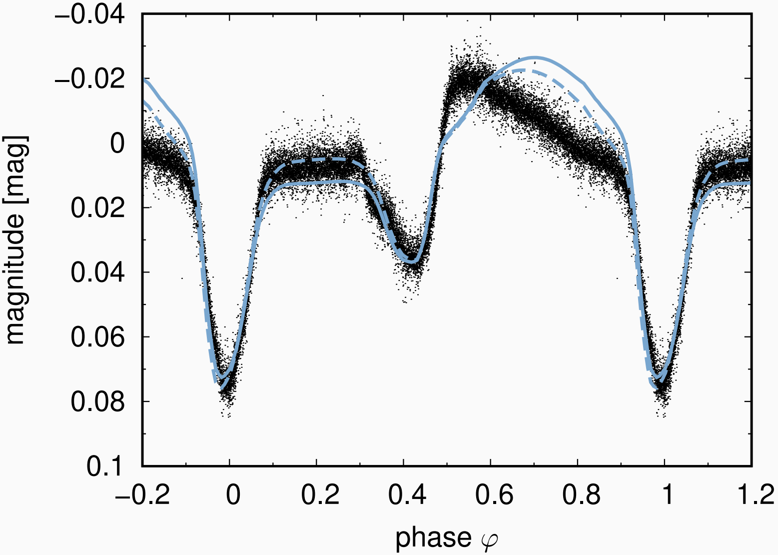

More complex field (tilted hexapole)

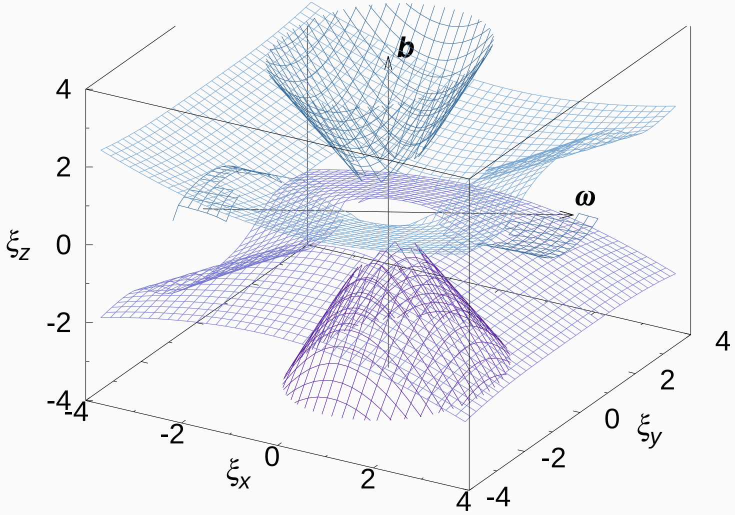

$n = 4$

Rotating magnetospheres: observables

Many quantities are variable in magnetic stars with rotating magnetospheres:

- Hα line emission (Sundqvist et al. 2012)
- visual photometry (Townsend et al. 2005, Wade et al. 2011, Krtička 2016)
- wind line profiles (Marcolino et al. 2013)
- continuum polarization (Carciofi et al. 2013)
- X-ray emission (Nazé et al. 2016)
- radio emission

Massive star in the plot of $R_\mathsf{A}/R_\mathsf{K}$ vs. luminosity

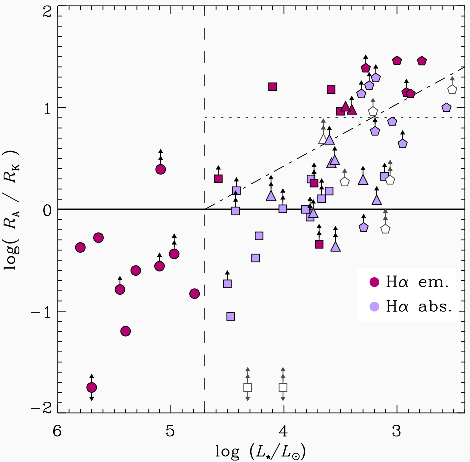

O stars: typically dynamical magnetospheres with Hα emission due to the winds. B stars: dynamical vs. centrifugal magnetospheres with Hα emission due to the circumstellar environment (Petit et al. 2013).

Open questions

- 3D MHD for non-axisymmetric cases (non-aligned magnetic fields)
- MHD modelling of higher order multipoles
- magnetospheric leakage (Owocki & Cranmer 2018)

Magnetic braking

Magnetic field in equatorial plane (spherical coordinates)

Frozen field condition for the ϕ component:
$\nabla \times (\boldsymbol{v} \times \boldsymbol{B}) = 0 \Rightarrow \frac{1}{r}\frac{\mathrm{d}}{\mathrm{d}r}\left[r(v_r B_\phi - v_\phi B_r)\right] = 0.$
By integrating and evaluating the constant at R_* where $v_r \ll v_\phi$: $r(v_r B_\phi - v_\phi B_r) = -R_*^2 \Omega B_{r,0}$.
Assuming $\boldsymbol{B} = \boldsymbol{B}(r)$ the Maxwell's equation $\nabla \cdot \boldsymbol{B} = 0$ gives $\mathcal{F}_B = r^2 B_r = R_*^2 B_{r,0}$ and

$$\frac{B_\phi}{B_r} = \frac{v_\phi - r\Omega}{v_r}.$$

Close to the star: $v_\phi \approx r\Omega$, $B_r \gg B_\phi$: solid body rotation. In outer regions: $v_\phi < r\Omega$, negative B_ϕ, no co-rotation.

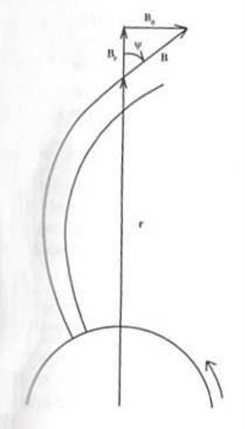

Wind equations in equatorial plane (spherical coordinates)

Momentum equation (neglecting the gas pressure)

$$\rho(\boldsymbol{v} \cdot \nabla)\boldsymbol{v} = -\rho g_* \hat{\boldsymbol{r}} \; + \; \rho g_{\mathrm{rad}} \hat{\boldsymbol{r}} + \frac{1}{4\pi}(\nabla \times \boldsymbol{B}) \times \boldsymbol{B}$$

has in the azimuthal direction the form of

$$\rho v_r \frac{\mathrm{d}}{\mathrm{d}r}\left(r v_\phi\right) = \frac{B_r}{4\pi}\frac{\mathrm{d}}{\mathrm{d}r}\left(r B_\phi\right).$$

From $\rho v_r r^2 = \mathrm{const.}$ and $r^2 B_r = \mathrm{const.}$ we derive

$$\frac{\mathrm{d}\mathcal{L}}{\mathrm{d}r} = 0,$$

where

$$\mathcal{L} = r v_\phi - \frac{r B_r B_\phi}{4\pi \rho v_r}.$$

Angular momentum carried by the gas and by the magnetic field is constant.

Angular momentum loss

Inserting $B_\phi = B_r(v_\phi - r\Omega)/v_r$ into equation for $\mathcal{L}$ we derive

$$v_\phi = r\Omega \frac{\frac{v_r^2 \mathcal{L}}{r^2\Omega} - v_\mathrm{A}^2}{v_r^2 - v_\mathrm{A}^2},$$

where the (radial) Alfvén speed is $v_\mathrm{A} = B_r/\sqrt{4\pi\rho}$. Azimuthal velocity finite at the Alfvén radius R_A where $v_r = v_\mathrm{A}$:

$$\mathcal{L} = R_\mathrm{A}^2 \omega.$$

Angular momentum (per unit of mass) behaves *as if* the star rotates as a solid body out to the Alfvén radius (Weber & Davis 1967, Lamers & Cassinelli 2000). Angular momentum due to the wind and magnetic stresses.

The spin down time

Stellar angular momentum loss $\dot{J} = \dot{M} R_A^2 \Omega$ gives with the stellar angular momentum $J = \eta M R_*^2 \Omega$ the spin down time

$$\tau_{\text{spin}} = \frac{J}{\dot{J}} \approx \frac{\eta M R_*^2}{\dot{M} R_A^2}.$$

For solar-type stars $\dot{M} = \dot{M}(\Omega)$ and $R_A = R_A(\Omega)$ and the Skumanich (1972) law holds: $\Omega \sim \sqrt{t}$.

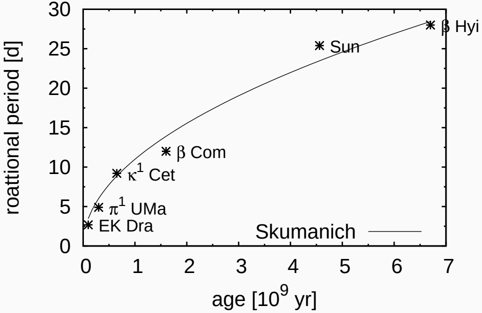

Ribas et al. (2005)

Spin down time in massive stars

With $R_\mathrm{A} \approx R_* \eta_*^{1/4}$ the spin down time in massive stars is from the numerical simulations (ud-Doula et al. 2009)

$$\tau_\mathrm{spin} \approx 1.1 \times 10^8\,\mathrm{yr}\,\frac{\eta}{\left(\frac{B_\mathrm{p}}{1\,\mathrm{kG}}\right)}\frac{\left(\frac{M}{1\,M_\odot}\right)}{\left(\frac{R_*}{R_\odot}\right)}\left[\frac{\left(\frac{v_\infty}{10^8\,\mathrm{cm\,s^{-1}}}\right)}{\left(\frac{\dot{M}}{10^{-9}\,M_\odot\,\mathrm{yr}^{-1}}\right)}\right]^{1/2}$$

Spin down time of σ Ori E 1.34 Myr (Townsend et al. 2010) agrees with 1.7 Myr predicted from theoretical wind models (Krtička 2014).

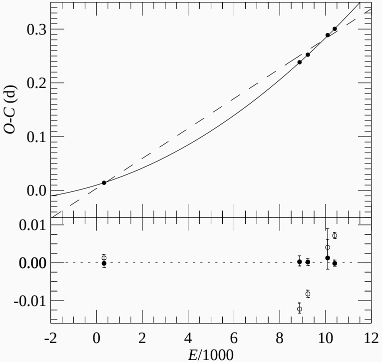

Radio emission & planets

Radio emission

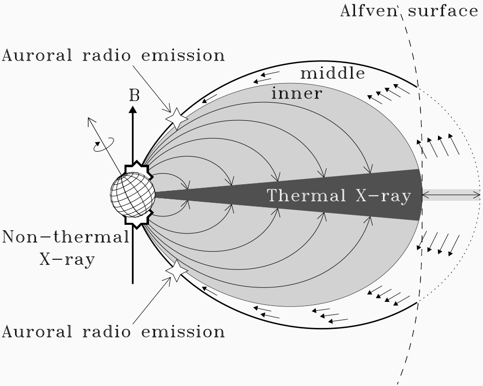

Collision of wind streams from oposite hemispheres: X-rays. Close to the Alfvén radius: magnetic reconnection, generation of fast electrons. Electrons propagate toward the star: gyrosynchrotron radiation. Collision of electrons withe stellar surface: reflected electron cause beamed auroral radio emission due to the coherent electron cyclotron maser emission.

(Leto et al. 2018)

Magnetospheres of giant planets

The rapid rotation of the gas giant planets, Jupiter and Saturn, leads to the formation of magnetodisc regions in their magnetospheric environments. In these regions, relatively cold plasma is confined towards the equatorial regions, and

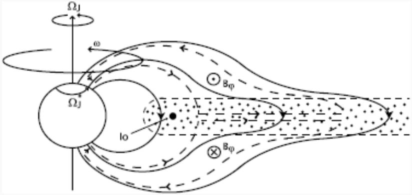

the magnetic field generated by the azimuthal (ring) current adds to the planetary dipole, forming radially distended field lines near the equatorial plane. The ensuing force balance in the equatorial magnetodisc is strongly influenced by centrifugal stress and by the thermal pressure of hot ion populations, whose thermal energy is large compared to the magnitude of their centrifugal potential energy. The sources of plasma for the Jovian and Kronian magnetospheres are the respective satellites Io (a volcanic moon) and Enceladus (an icy moon).

(Achilleos et al. 2015)

Magnetospheres of giant planets

Magnetodisks: rapid rotation + small angle between the magnetic and rotational axes. Directly observed by spacecrafts (e.g., *Voyager, Galileo, Cassini*).

(Achilleos et al. 2015)

Saturn: auroral emission from the boundary between open and closed field lines due to interaction of magnetosphere and solar wind.

(Bunce et al. 2008)

Jupiter: radio emission due to synchrotron radiation of relativistic electrons.

(Chang & Davis 1962)

Magnetospheres of acreting stars

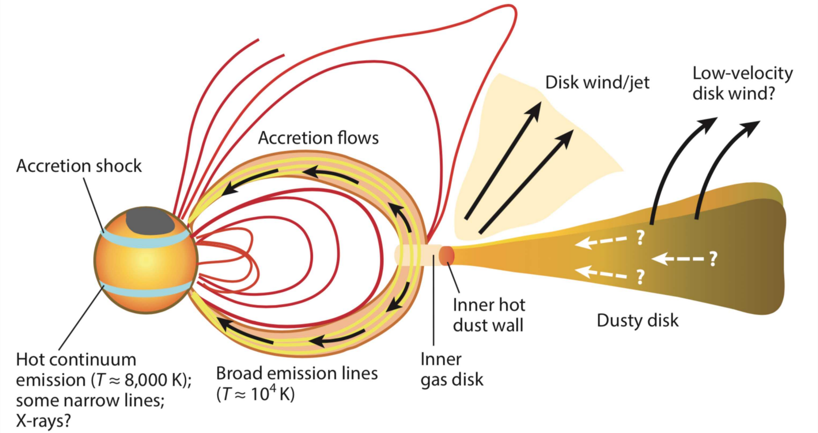

(Hartmann 2016)